Negative nonlinear susceptibility of cesium vapor around 1.06 μm*

R. H. Lehmberg, J. Reintjes, and R. C. Eckardt
Naval Research Laboratory, Washington, D.C. 20375
(Received 16 June 1975; revised manuscript received 1 October 1975)

We outline a complete theory of the nonlinear susceptibility of cesium around 1.06 μm, and present the first measurements of the negative nonlinear refractive index n_2 primarily responsible for the self-defocusing that is observed. For linearly polarized light, our measured value of n_2 is $-(1.4 \pm 0.2) \times 10^{-30} N$ esu, where N is the atomic density. This is in reasonable agreement with our calculated value of $-2.62 \times 10^{-30} N$. The main portion of n_2 comes from a two-photon resonance between the $6s$ and $7s$ levels, and an additional negative term arises from induced population changes between $6s$ and $6p$. For circular polarization, n_2 arises mainly from the induced population changes, giving the measured and calculated values of $(0.26 \pm 0.03) \times 10^{-30} N$ and $-0.525 \times 10^{-30} N$, respectively. In our experiments where the 35-psec pulses were shorter than the $6s$-$6p$ inverse linewidth, the nonlinear susceptibility depends mainly on the instantaneous intensity; however, for longer pulses, one would obtain additional contributions proportional to time integrals over the intensity. Since the useful output power from large Nd laser systems is limited by self-focusing due to the laser glass, our results suggest the possibility of increasing this power by using Cs vapor for compensation.

I. INTRODUCTION

In recent years, a number of authors have observed self-focusing,[1-4] self-defocusing,[5] and other related effects[6,7] owing to a resonant enhancement of the electronic nonlinear susceptibility in atomic vapors. These effects arise from optically induced population changes associated with single-photon[1-3,5-7] or two-photon[4] absorption.

Recently, we reported the observation of self-defocusing of mode-locked 1.06-μm pulses in cesium vapor.[8] For linearly polarized light, we attributed this primarily to a two-photon resonant enhancement of the third-order nonlinear susceptibility.[9] This contribution leads to an intensity-dependent refractive index

$$\delta n^{(3)}(t) \sim n_2 I(t) \sim I(t)/(\omega_{20} - 2\omega) ,$$

where n_2 is the nonlinear refractive index and ω and ω_{20} are, respectively, the optical frequency and the near-resonant atomic frequency. In cesium vapor around $\lambda = 1.06$ μm, 2ω lies slightly above the $6s$-$7s$ frequency; hence $n_2 < 0$, and at pressures of a few Torr its magnitude is comparable to that of laser glass.[10] Since the useful output power from large Nd laser systems is ordinarily limited by self-focusing in the glass amplifiers, the existence of a negative n_2 at 1.06 μm raises the possibility of increasing this power by using Cs vapor for compensation.

The nonlinear behavior of Cs is complicated somewhat by additional self-defocusing contributions arising primarily from pulse-induced population changes in the $6s$ and $6p$ levels. For pulse widths t_p short in comparison to the $6s$-$6p$ dephasing time Γ_{10}^{-1}, this effect remains intensity dependent,[1,5] and for linearly polarized light, its contribution to n_2 is relatively small; however, as a result of atomic collisional relaxation, it can also contribute terms proportional to time integrated intensities,[11] and these "inertial" terms can easily predominate if $t_p \gg \Gamma_{10}^{-1}$. The result is then similar to thermal defocusing.[12]

In this paper, we outline a complete theory of the third-order nonlinear refractive index $\delta n^{(3)}(t)$, and relate this to earlier theoretical work.[11,13-15] We then describe the first measurements of n_2 in Cs vapor at 1.064 μm under conditions where the instantaneous terms are expected to predominate, and compare these results to the theory.

Assuming only that t_p is short in comparison to the atomic radiative lifetimes, and that ω and 2ω lie outside the atomic line profiles, we show that $\delta n^{(3)}(t)$ can always be expressed as the sum of instantaneous and inertial contributions. The inertial terms derived here include the effects of excited-state collisional mixing (e.g., among the $6p$ sublevels) in addition to atomic phase relaxation. Specializing to a three-level model applicable to Cs around 1.06 μm,[8] we then derive simple approximate expressions for the two-photon and induced-population terms described above. In particular, we show that the $6s$-$7s$ two-photon term disappears if the light is circularly polarized.

The measurements of n_2 were carried out by observing the self-defocusing of linearly and circularly polarized mode-locked pulses in a cesium cell. We also measured the insertion loss of the cesium at different peak intensities, and found a broad minimum (<5% absorption) centered

around 5 GW/cm^2. The measured values of n_2 are $-(1.4\pm0.2)\times10^{-30}N$ esu for linear polarization and $-(0.26\pm0.03)\times10^{-30}N$ esu for circular polarization, in reasonable agreement with the calculated values of $-2.62\times10^{-30}N$ and $-0.525\times10^{-30}N$, respectively.

II. THEORY

A. Basic equations

The lowest-order nonlinear refractive properties of an isotropic medium can be found from the polarization

$$\vec{P}^{(3)}(t)=N\sum_{\alpha,\beta}\vec{\mu}_{\beta\alpha}\rho^{(3)}_{\alpha\beta}(t) \tag{1}$$

induced by the optical field

$$\vec{E}(t)=\tfrac{1}{2}\hat{\epsilon}\,\mathcal{E}(\omega,t)e^{-i\omega t}+\tfrac{1}{2}\hat{\epsilon}^*\mathcal{E}(-\omega,t)e^{+i\omega t}. \tag{2}$$

Here N is the atomic density, $\vec{\mu}_{\beta\alpha}=e\vec{r}_{\beta\alpha}$ are the atomic dipole matrix elements between states $|\alpha\rangle$ and $|\beta\rangle$, $\rho^{(3)}_{\alpha\beta}(t)$ are the corresponding third-order density matrix elements, $\mathcal{E}(\omega,t)=[\mathcal{E}(-\omega,t)]^*$ is the slowly varying optical field amplitude, and $\hat{\epsilon}$ is a unit vector defining the optical polarization state. The density matrix elements are obtained by solving the Boltzmann equations

$$\dot{\rho}^{(n)}(t)=-(i/\hbar)[H_0,\rho^{(n)}(t)]-(i/\hbar)[V(t),\rho^{(n-1)}(t)]+\{\dot{\rho}^{(n)}(t)\}_R, \tag{3}$$

for $n=1,2,3$, subject to the condition $\rho^{(0)}_{00}=1$. Here

$$H_0=\sum_\alpha\hbar\omega_{\alpha0}|\alpha\rangle\langle\alpha|,$$
$$V(t)=-\sum_{\alpha,\beta}\vec{E}(t)\cdot\vec{\mu}_{\alpha\beta}|\alpha\rangle\langle\beta|, \tag{4}$$

$|0\rangle$ is the ground state, $\hbar\omega_{\alpha0}$ is the energy difference between $|\alpha\rangle$ and $|0\rangle$, and $\{\dot{\rho}^{(n)}(t)\}_R$ describes the atomic relaxation. If we write $\rho^{(3)}_{\alpha\beta}(t)$ in terms of its slowly varying amplitudes, $\sigma^{(3)}_{\alpha\beta}(\omega,t)=[\sigma^{(3)}_{\beta\alpha}(-\omega,t)]^*$,

$$\rho^{(3)}_{\alpha\beta}(t)=\tfrac{1}{2}\sigma^{(3)}_{\alpha\beta}(\omega,t)e^{-i\omega t}+\tfrac{1}{2}\sigma^{(3)}_{\alpha\beta}(-\omega,t)e^{+i\omega t}+(\text{third-harmonic terms}), \tag{5}$$

then the nonlinear contribution to the refractive index of an isotropic medium is

$$\delta n^{(3)}(t)=2\pi N\sum_{\alpha,\beta}\hat{\epsilon}^*\cdot\vec{\mu}_{\beta\alpha}\frac{\sigma^{(3)}_{\alpha\beta}(\omega,t)}{\mathcal{E}(\omega,t)}. \tag{6}$$

The following two simplifications are assumed to be valid throughout the remainder of this paper: (i) One can ignore all longitudinal relaxation processes, except for collisional mixing among the excited levels, and (ii) the atomic and laser linewidths are negligible in comparison to the detuning frequencies $|\omega_{\alpha\beta}-\omega|$ and $|\omega_{\alpha\beta}-2\omega|$ that arise in the expression for $\delta n^{(3)}(t)$. Condition (i), which is generally necessary to avoid optical pumping effects,[16] requires that the laser pulsewidth t_p be short in comparison to the radiative lifetimes of the excited states. Condition (ii) is well satisfied for cesium vapor around 1.06 μm with $N\leq10^{19}$ cm^{-3} and laser linewidths up to several angstroms.

The resulting solution of Eqs. (1)–(6), which is outlined in the appendix, yields the expression

$$\delta n^{(3)}(t)=\delta n'(t)+\delta n''(t) \tag{7a}$$
$$=n_2\langle E^2(t)\rangle+2\pi N\sum_{\alpha>\beta}\chi_{\alpha\beta}[q_\beta(t)-q_\alpha(t)]. \tag{7b}$$

In $\delta n'(t)$, the nonlinear refractive index is

$$n_2\equiv\frac{2\pi N}{\hbar}\sum_{\beta\neq0}\left(\frac{|P^-_\beta|^2}{\omega_{\beta0}-2\omega}+\frac{|P^+_\beta|^2}{\omega_{\beta0}+2\omega}+\frac{|Q_\beta|^2}{\omega_{\beta0}}\right)-2\pi N\left(Q_0\sum_\alpha R_\alpha+\frac{|P^-_0|^2-|P^+_0|^2}{2\hbar\omega}\right), \tag{8}$$

where

$$P^-_\beta\equiv\sum_\alpha\frac{\hat{\epsilon}\cdot\vec{\mu}_{\beta\alpha}\hat{\epsilon}\cdot\vec{\mu}_{\alpha0}}{\hbar(\omega_{\alpha0}-\omega)},\quad P^+_\beta\equiv\sum_\alpha\frac{\hat{\epsilon}^*\cdot\vec{\mu}_{\beta\alpha}\hat{\epsilon}^*\cdot\vec{\mu}_{\alpha0}}{\hbar(\omega_{\alpha0}+\omega)}, \tag{9a}$$

$$Q_\beta\equiv\sum_\alpha\left[\frac{\hat{\epsilon}^*\cdot\vec{\mu}_{\beta\alpha}\hat{\epsilon}\cdot\vec{\mu}_{\alpha0}}{\hbar(\omega_{\alpha0}-\omega)}+\frac{\hat{\epsilon}\cdot\vec{\mu}_{\beta\alpha}\hat{\epsilon}^*\cdot\vec{\mu}_{\alpha0}}{\hbar(\omega_{\alpha0}+\omega)}\right], \tag{9b}$$

$$R_\alpha\equiv\frac{|\hat{\epsilon}\cdot\vec{\mu}_{\alpha0}|^2}{\hbar^2(\omega_{\alpha0}-\omega)^2}+\frac{|\hat{\epsilon}^*\cdot\vec{\mu}_{\alpha0}|^2}{\hbar^2(\omega_{\alpha0}+\omega)^2}, \tag{9c}$$

and the bracket $\langle\,\rangle$ denotes an average over an optical cycle [i.e., $\langle E^2(t)\rangle=\frac{1}{2}|\mathcal{E}(\omega,t)|^2$]. In $\delta n''(t)$,

$$\chi_{\alpha\beta}\equiv\frac{|\hat{\epsilon}\cdot\vec{\mu}_{\alpha\beta}|^2}{\hbar(\omega_{\alpha\beta}-\omega)}+\frac{|\hat{\epsilon}^*\cdot\vec{\mu}_{\alpha\beta}|^2}{\hbar(\omega_{\alpha\beta}+\omega)} \tag{10}$$

is a linear susceptibility, the quantities $q_\alpha(t)$ are solutions of the rate equations

$$\dot{q}_\alpha(t)=-W_\alpha q_\alpha(t)+\sum_{\beta\neq\alpha}W_{\beta\alpha}q_\beta(t)+S_\alpha\langle E^2(t)\rangle \tag{11}$$

subject to the initial conditions $q_\alpha(-\infty)=0$, the driving terms are

$$S_\alpha\equiv(\Gamma_{\alpha0}-\tfrac{1}{2}W_\alpha)R_\alpha+\sum_{\beta\neq\alpha}\tfrac{1}{2}W_{\beta\alpha}R_\beta,\quad\alpha\neq0, \tag{12a}$$

$$S_0\equiv-\sum_{\alpha\neq0}\Gamma_{\alpha0}R_\alpha, \tag{12b}$$

$\Gamma_{\alpha0}$ is the homogeneous relaxation rate of $\rho_{\alpha0}(t)$,

and $W_{\beta\alpha}$ is the $\beta \to \alpha$ collisional mixing rate, which satisfies the conditions

$$W_{\beta\alpha} = W_{\alpha\beta} e^{-\hbar\omega_{\alpha\beta}/kT}, \tag{13a}$$

$$W_\alpha \equiv \sum_\beta W_{\alpha\beta} \leq 2\Gamma_{\alpha 0}, \tag{13b}$$

where $W_{\alpha\beta} = 0$ if α or β are zero. From Eqs. (11), (12), (13b), and the initial condition $q_\alpha(-\infty) = 0$, we obtain the useful identity

$$\sum_\alpha q_\alpha = 0. \tag{14}$$

The instantaneous term $\delta n'(t)$ is equivalent to the results obtained from the usual third-order perturbation theory,[13-15] while $\delta n''(t)$ arises from a change in the total susceptibility as a result of *incoherent* population of the excited levels. According to Eq. (A8), the total population change $\sigma^{(2)}_{\alpha\alpha}(0,t)$ consists of an instantaneous (coherent) portion plus the inertial (incoherent) portion $q_\alpha(t)$ that arises from atomic relaxation. The coherent contributions, which can be explained in terms of Grischkowsky's adiabatic following model,[1,5] are included in expression (8). Butylkin *et al.*[11] have derived results similar to ours, but their interpretation is different. In their formalism, our $q_\alpha(t)$ would represent the *total* population change, while the coherent population terms would be included *ad hoc* by inserting Stark-shift terms in the off-diagonal density matrix equations.

For short pulses (i.e., $\Gamma_{\alpha 0} t_p \ll 1$), the inertial terms are negligible, and Eq. (7) reduces to

$$\delta n^{(3)}(t) \simeq \delta n'(t) = n_2 \langle E^2 \rangle . \tag{15}$$

At the opposite extreme, $\Gamma_{\alpha 0} t_p \gg 1$, and

$$\delta n^{(3)}(t) \simeq \delta n''(t). \tag{16}$$

The expression for $\delta n''(t)$ can be simplified in the second case by noting that collisional mixing occurs only among the sublevels of each nl manifold. Since the mixing rates W_β are usually comparable to $\Gamma_{\alpha\beta}$,[17] these sublevels are completely thermalized if $\Gamma_{\alpha 0} t_p \gg 1$.

B. Three-level model

The theory presented so far is applicable to all atomic vapors under suitable conditions. For cesium vapor around 1.06 μm, one can obtain a useful and instructive approximation to this theory by examining the lower lying energy levels, shown in Fig. 1.[18] Around 1.06 μm, $\delta n^{(3)}$ appears to be determined mainly by the $|6s\rangle \equiv |0\rangle$, $|6p\rangle \equiv |1\rangle$, and $|7s\rangle \equiv |2\rangle$ levels because of the nearby one- and two-photon resonances with $6p$ and $7s$, respectively (i.e., $\omega_{10} - \omega \ll \omega_{10} + \omega$, and $|\omega_{20} - 2\omega| \ll \omega_{20}$). To a first approximation, we can therefore ignore all other levels and all nonresonant contributions to $\delta n^{(3)}(t)$. We will also ignore the L-S splitting of the $6p$ level, and approximate $6p$ by the degenerate magnetic substates $|a\rangle$, $|b\rangle$, $|c\rangle$ representing $m = +1$, 0, -1, respectively. This appears to be reasonable at 1.064 μm, where $(\omega_{10} - \omega)/2\pi c = 2149$ cm^{-1} and the L-S splitting is only 544 cm^{-1}. The error that this causes in the evaluation of n_2 is small in comparison to that caused by the neglect of higher-energy states and nonresonant contributions.

For linearly polarized light, we choose $\hat{\epsilon} \equiv \hat{z}$; hence the only nonvanishing matrix elements of interest are $\hat{z} \cdot \vec{\mu}_{b0} \equiv \mu_{10} = \mu^*_{10}$ and $\hat{z} \cdot \vec{\mu}_{2b} \equiv \mu_{21} = \mu^*_{21}$. Using the simplifications described above, one can approximate Eqs. (7)–(10) by

$$\delta n^{(3)}(t) \simeq n_2 \langle E^2(t) \rangle + \frac{2\pi N \mu_{10}^2}{\hbar(\omega_{10} - \omega)} [q_0(t) - q_b(t)] + \frac{2\pi N \mu_{21}^2}{\hbar(\omega_{21} - \omega)} q_b(t), \tag{17}$$

where

$$n_2 = n_{20} - n_{10} \tag{18a}$$

$$= \frac{2\pi N \mu_{21}^2 \mu_{10}^2}{\hbar^3(\omega_{10} - \omega)^2(\omega_{20} - 2\omega)} - \frac{2\pi N \mu_{10}^4}{\hbar^3(\omega_{10} - \omega)^3}, \tag{18b}$$

and $q_0(t)$ and $q_b(t)$ are solutions of Eq. (11). The term $q_2(t)$ has not been included in (17) because it is fourth order in $E(t)$, and is therefore negligible unless $\omega_{20} - 2\omega$ is comparable to the atomic linewidth. Such terms were discussed by Butylkin

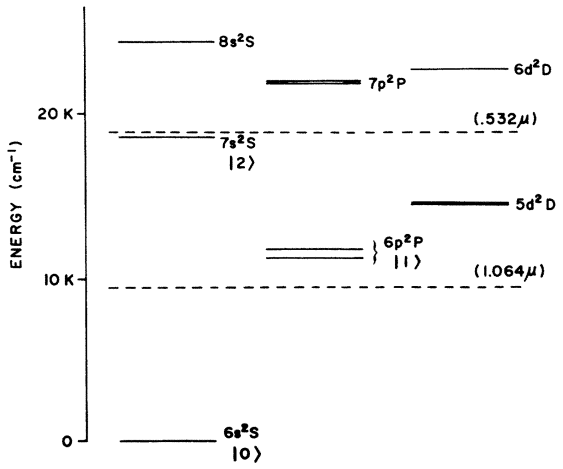

FIG. 1. Energy-level diagram of Cs, showing the three levels $|6s\rangle \equiv |0\rangle$, $|6p\rangle \equiv |1\rangle$, and $|7s\rangle \equiv |2\rangle$ primarily responsible for self-defocusing at 1.064 μm. The dotted lines show the position of the laser fundamental at 1.064 μm and its two-photon level at 0.532 μm.

et al.,[11] and have recently been observed in potassium vapor.[4]

The neglect of L-S splitting allows one to obtain simple expressions for $q_0(t)$ and $q_b(t)$ with only two relaxation constants. By symmetry considerations, it follows that $\Gamma_{a0}=\Gamma_{b0}=\Gamma_{c0}\equiv\Gamma_{10}$, $W_a=W_b=W_c\equiv W$, and $W_{\alpha\beta}=\frac{1}{2}W$ for $\alpha\neq\beta$ equal to a, b, or c. Equation (11) then reduces to

$$\dot{q}_0\simeq-[\Gamma_{10}\mu_{10}^2/\hbar^2(\omega_{10}-\omega)^2]\langle E^2\rangle \tag{19a}$$

$$\dot{q}_b\simeq-\tfrac{3}{2}Wq_b-\tfrac{1}{2}Wq_0+(\Gamma_{10}-\tfrac{1}{2}W)[\mu_{10}^2/\hbar^2(\omega_{10}-\omega)^2]\langle E^2\rangle\ , \tag{19b}$$

where the identity $q_0+q_a+q_b+q_c=0$ [Eq. (14)] has been used to obtain (19b). Solving for $q_0(t)$ and $q_b(t)$, and substituting them into (17), we obtain the result

$$\delta n^{(3)}(t)\simeq n_2\langle E^2(t)\rangle+C_1\int_{-\infty}^{t}\langle E^2(t')\rangle\,dt'+C_2\int_{-\infty}^{t}e^{-(3/2)W(t-t')}\langle E^2(t')\rangle\,dt'+C_3\int_{-\infty}^{t}e^{-(3/2)W(t-t')}\,dt'\int_{-\infty}^{t'}\langle E^2(t'')\rangle\,dt'', \tag{20}$$

$$C_1\equiv-\Gamma_{10}n_{10}\,, \tag{21a}$$

$$C_2\equiv-(\Gamma_{10}-\tfrac{1}{2}W)(n_{10}-n_{21})\,, \tag{21b}$$

$$C_3\equiv-\tfrac{1}{2}W\Gamma_{10}(n_{10}-n_{21})\,, \tag{21c}$$

and

$$n_{21}\equiv\frac{2\pi N\mu_{21}^2\mu_{10}^2}{\hbar^3(\omega_{10}-\omega)^2(\omega_{21}-\omega)}\,. \tag{22}$$

As we indicated in Sec. IIA, the integral terms arise from incoherent redistribution of the $6s$ and $6p$ populations, and will predominate if $\Gamma_{10}t_p\gg1$.

For pulse widths comparable to or less than the atomic relaxation times Γ_{10}^{-1} and W^{-1}, the most important contribution to $\delta n^{(3)}(t)$ is the two-photon term n_{20} defined by Eqs. (18), as we will show at the end of this section. This term is positive in most substances around 1.06 μm, and is partially responsible for the self-focusing observed in materials such as laser glass.[19] In Cs vapor around 1.06 μm, however, n_{20} is large and negative due to the strong resonant enhancement by the two-photon denominator $(\omega_{20}-2\omega)/2\pi c=-261\ \mathrm{cm}^{-1}$.

The instantaneous portion of $\delta n^{(3)}(t)$ can be interpreted physically by rewriting expression (18b) in the form[8]

$$n_2=\frac{\pi N\mu_{21}^2\mu_{10}^2}{\hbar^3(\omega_{20}-2\omega)(\omega_{10}-\omega)}\left(\frac{1}{\omega_{10}-\omega}-\frac{1}{\omega_{21}-\omega}\right)-\frac{\pi N\mu_{10}^2}{\hbar^3(\omega_{10}-\omega)^2}\left(\frac{2\mu_{10}^2}{\omega_{10}-\omega}-\frac{\mu_{21}^2}{\omega_{21}-\omega}\right). \tag{23}$$

The first (and largest) pair of terms arises directly from the two-photon "polarization" $\sigma_{20}^{(2)}(2\omega)$, which drives $\sigma_{10}^{(3)}(\omega)$ and $\sigma_{21}^{(3)}(\omega)$. The second pair arises from the coherent redistribution of the $6s$ and $6p$ populations, as described by adiabatic following theory.[1,5] We have recently shown that the combined coherent and incoherent population terms in a two-level system (i.e., in the absence of μ_{21} and W) can be described by a generalized adiabatic following approximation that takes account of the phase relaxation Γ_{10}.[20]

For circularly polarized light, we choose $\hat{\epsilon}=\hat{r}^+\equiv2^{-1/2}(\hat{x}+i\hat{y})$; hence the only nonvanishing matrix elements of interest are $\hat{r}^+\cdot\vec{\mu}_{a0}=\mu_{10}=\mu_{10}^*$ and $\hat{r}^+\cdot\vec{\mu}_{2c}=\mu_{21}=\mu_{21}^*$. The magnitudes of μ_{10} and μ_{21} are equal to those in the linearly polarized case. Using the same approximations and procedure as above, we again obtain Eq. (20), but the constants n_2 and C_2 are now defined by

$$n_2=-n_{10}\,, \tag{24}$$

$$C_2=-(\Gamma_{10}-\tfrac{1}{2}W)n_{10}+\tfrac{1}{4}Wn_{21}\,. \tag{25}$$

The n_{20} term does not appear in this case because the corresponding virtual transition $6s\rightarrow6p\rightarrow7s$

TABLE I. $(n_2/N)\times10^{30}$ (esu).

Polarization	Experimental		Theoretical		Miles and Harris
Linear	-1.5 ± 0.02 [a]	-1.4 ± 0.2 [b]	-2.70 [c]	-2.62 [d]	-0.66 [e]
Circular	-0.35 ± 0.04 [a]	-0.26 ± 0.03 [b]	-0.335 [c]	-0.525 [d]	...

[a] Experimental values obtained from analysis of data that ignores the integral terms of Eq. (20).
[b] Experimental values including an adjustment to account approximately for the integral terms.
[c] Theoretical calculation using the near-resonant three-level approximation [Eqs. (18) and (24)].
[d] Theoretical calculation including antiresonant terms, higher excited states, and L-S splitting [Eq. (8)].
[e] Theoretical calculation of Ref. 23.

requires zero net angular momentum transfer from the light to the atom, whereas two photons of circularly polarized light must transfer $\Delta J = \pm 2$.[21] (Two-photon contributions do arise from the n^2D levels, but they have not been included in this simple approximation.) From Eq. (24) and definitions (18a) and (18b), we see that n_2 reduces to the expression derived by Grischkowsky,[1,5] as one would expect in this case.

To evaluate n_{20}, n_{10}, and n_{21}, we used matrix elements obtained from the total $6s^2S_{1/2}$-$6p^2P_{1/2,\,3/2}$ and $6p^2P_{1/2,\,3/2}$-$7s^2S_{1/2}$ line strengths calculated by Heavens,[22] and took the energy of $6p$ to be 11 547 cm^{-1} (the weighted average of $6p^2P_{1/2}$ and $6p^2P_{3/2}$). The magnitudes of the matrix elements are (in atomic units) $|\mu_{10}| = 3.16$ and $|\mu_{21}| = 2.92$, giving the results $n_{20} = -2.36 \times 10^{-30} N$, $n_{10} = 0.335 \times 10^{-30} N$, and $n_{21} = -0.256 \times 10^{-30} N$ esu for $\lambda = 1.064$ μm. The resulting values of n_2 obtained from Eqs. (18) and (24) for linear and circular polarization, respectively, are shown in the third column of Table I. In the fourth column, we show the values of n_2 calculated from the exact expression [Eq. (8)], taking account of the contributions from nonresonant terms and higher-lying states (up to $8s$, $8p$, and $6d$), and including the effects of L-S splitting. The magnitudes of the matrix elements were again calculated from Heavens's data,[22] while the signs were taken from Table I of Miles and Harris.[23]

In the case of linear polarization, the good agreement between the third and fourth columns of Table I justifies our simple three-level model. The small discrepancy arises primarily from the contribution of the $7p$ levels in the exact expression. For circular polarization, the discrepancy is significantly larger, and stems primarily from the two-photon $6s$-$5d$ and $6s$-$6d$ contributions that were not included in the three-level model.

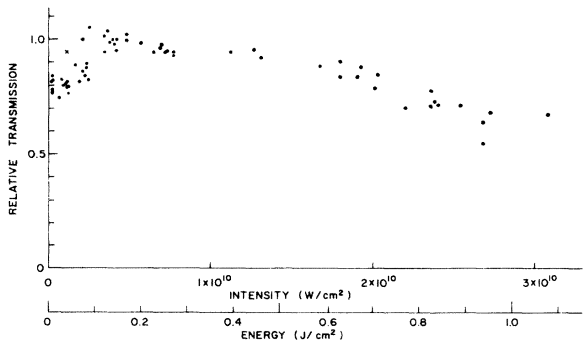

FIG. 2. Cesium transmission vs pulse flux (and peak intensity) for linearly polarized light and atomic density 0.32×10^{17} cm^{-3}.

III. EXPERIMENT

In order to measure n_2, we studied the self-defocusing of mode-locked Nd:YAG pulses in a 100-cm-long cesium vapor cell. The measurements were made at several densities between $N = 0.08 \times 10^{17}$ and 0.32×10^{17} cm^{-3} with linearly polarized pulses and at 0.32×10^{17} cm^{-3} with circular polarization. The density was controlled by adjusting the temperature of a cesium reservoir (260–305 °C), while the main cell was held at 460 °C in order to minimize linear absorption from Cs dimers.[24] For $N = 0.32 \times 10^{17}$ cm^{-3}, the $6s$-$6p$ transverse relaxation time Γ_{10}^{-1} is approximately 80 psec.

The input radiation consisted of single pulses of full width at half-maximum (intensity) duration $t_p = 35$ psec, as determined by measurements with a 5-psec-resolution streak camera. Since $\Gamma_{10}^{-1} > 2t_p$ at all Cs pressures, the instantaneous terms are expected to predominate in Eqs. (7) and (20); hence expression (15) should be a good approximation, at least for the linearly polarized pulses. The input beam, which was well collimated (radius of curvature $\rho_0 \simeq 20$ m), had the form of an Airy profile truncated at the first minimum, with a $1/e$ intensity radius of $a_0 = 0.58$ mm. The pulse energy entering the cell was measured with a calorimeter, and was monitored with a calibrated photodiode. For the linear polarization case, simultaneous energy measurements were made at the output to determine the transmission of the cesium, which is plotted versus input pulse energy in Fig. 2.

The energy profile at the output of the cell was recorded by imaging the exit window onto a silicon photodiode array of 25-μm resolution. Figure 3(a) shows typical oscilloscope traces of these output profiles for the case $N = 0.32 \times 10^{17}$ cm^{-3}. At low intensities, the beam profile was identical to that obtained with linear propagation in an empty cell. At intermediate intensities, the beam size increased, but its smooth characteristic shape was retained. At the highest intensities used, further increase in beam size was observed, accompanied by beam distortion and the appearance of ring structure near the axis. This behavior is similar to that observed in the self-defocusing experiments of Grischkowsky and Armstrong.[5] All of the data that was used in determining n_2 was taken at the intermediate intensities (≈ 6 GW/cm^2) where the beam distortion and cesium insertion loss were negligible.

In analyzing the data, we calculated the output profile of the beam from a solution of the wave equation in the paraxial-ray approximation. Using Eq. (15), along with a constant-shape assumption,[12] and approximating the shape of the input beam with

a Gaussian distribution, we obtain for the intensity profile at the end of the cell

$$I(r,t)=[P(t)/\pi a^2(t)]\exp[-r^2/a^2(t)]\,. \tag{26}$$

Here $P(t)$ is the input beam power and $a(t)$ is a time-dependent radius given by[12]

$$a^2(t)=a_0^2\{(1+z/\rho_0)^2+[1-P(t)/P_c](\lambda z/2\pi a_0^2)^2\}\,, \tag{27}$$

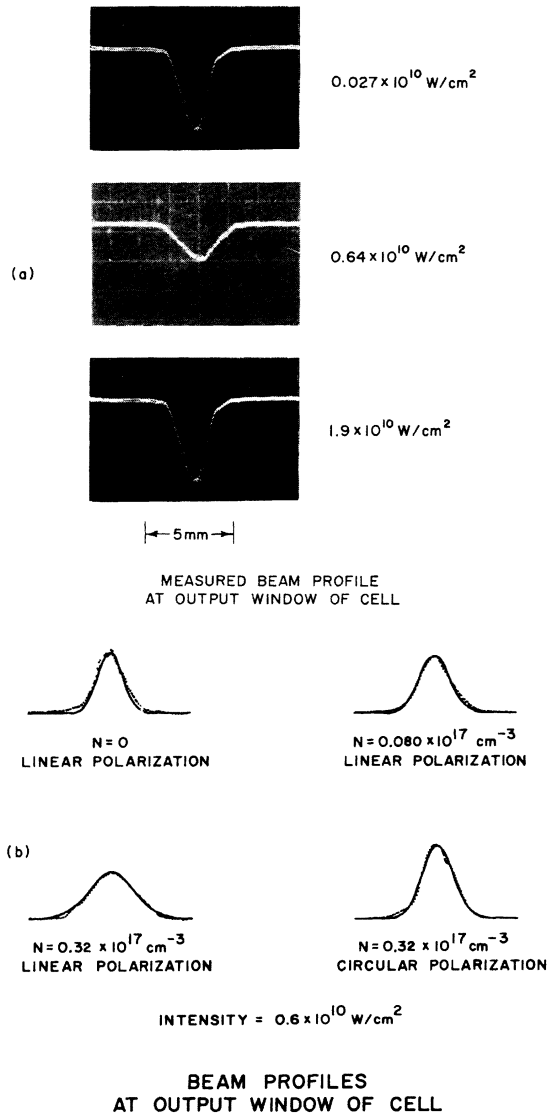

FIG. 3. Spatial profiles of the pulse at the exit window of the Cs cell. (a) Oscilloscope traces of photodiode array measurement at low, intermediate, and high intensity. (b) Comparison between theoretical profiles (solid lines) and typical measured profiles (dotted lines) at intermediate pulse energies.

where z is the length of the Cs cell, a_0 and ρ_0 are the input radius and beam curvature, respectively, and $P_c \equiv \lambda^2 c/32\pi^2 n_2 < 0$. The energy profile was then obtained by numerically integrating expression (26) over the pulse duration. For each data point, measured values of a_0, ρ_0, and $P(t)$ were used and the value of n_2 was chosen to give the best theoretical fit to the measured energy distribution at the half-maximum points. This procedure is justified by the good overall agreement between the calculated and experimental profiles, as illustrated by the examples shown in Fig. 3(b).

IV. RESULTS AND DISCUSSION

The results of our n_2 measurements for linearly and circularly polarized light are shown as a function of density in Fig. 4, and are compared with the theory in Table I. The first column of Table I gives the experimental values of n_2/N obtained using Eqs. (15), (26), and (27), as described above. The second column gives adjusted experimental values which account approximately for the contribution of the integral terms in Eq. (20), as we will discuss below. The third and fourth columns give the approximate and exact calculated values of n_2/N that were discussed in Sec. II, and the last column gives the value obtained from the susceptibility calculations of Miles and Harris.[23]

In using Eq. (15) to analyze the data, we have, in effect, treated the small integral terms of $\delta n^{(3)}(t)$ [Eq. (20)] as instantaneous, and lumped them into an effective contribution to the measured value of n_2. One can estimate the relative importance of these integral terms by averaging their contribution to $\delta n^{(3)}(t)$ over the incident intensity, and comparing this to a similar average

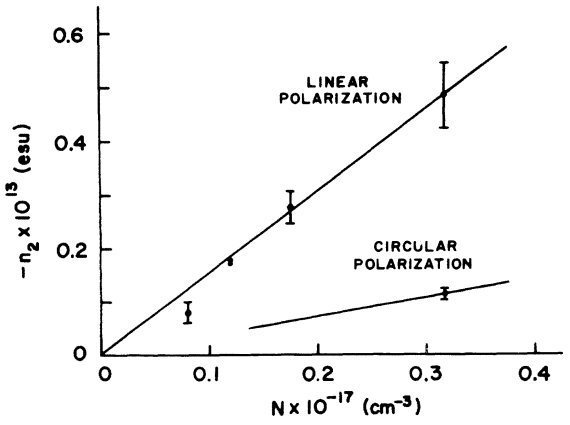

FIG. 4. Effective nonlinear refractive index n_2 vs atomic density N for linearly and circularly polarized light at 1.064 μm.

of the instantaneous portion; i.e., we consider the quantity

$$\eta \equiv \frac{\int_{-\infty}^{\infty} [\delta n^{(3)}(t) - n_2\langle E^2(t)\rangle]\langle E^2(t)\rangle\, dt}{\int_{-\infty}^{\infty} n_2 \langle E^2(t)\rangle^2\, dt}, \tag{28}$$

using Eq. (20) and the exact values of n_2 from the fourth column of Table I. The corrected values of n_2 would then be approximately $(1+\eta)^{-1}$ times the numbers shown in the first column. Assuming that $\Gamma_{10}^{-1} \simeq 80$ psec,[25] and that $W \approx \Gamma_{10}$,[17] we obtain $\eta(\text{linear}) \simeq 0.08$ and $\eta(\text{circular}) \simeq 0.36$ by numerical integration of Eq. (28). Integral terms thus contribute little in the case of linear polarization, but they result in a significant correction for circular polarization, where $|n_2|$ is relatively small.

The experimental and theoretical values of n_2 (second and fourth columns of Table I) are in reasonable agreement, considering that one is comparing *ab initio* calculations with absolute measurements. Since the oscillator strengths corresponding to our matrix elements are probably too large by a factor of about 5%,[22] the numbers in the third and fourth columns could be overestimated by as much as 10%; hence the actual discrepancy between theory and measurements is probably smaller than indicated in Table I. The remaining discrepancy appears to arise from systematic errors in the values of the concentration N or the pulse power $P(t)$. N was obtained from vapor-pressure tables[26] and the measured temperatures of the bulb and cell. As other authors have noted,[5] the accuracy of this procedure is limited. In the ratio $n_2(\text{linear})/n_2(\text{circular})$ the factor N cancels, and the agreement between theory and measurements is within 8% (i.e., the ratio is 5.4 from the second column of Table I and 5.0 from the fourth column).

Although the cesium insertion loss was negligible for the pulses used in the n_2 measurements, its existence at higher and lower intensities (Fig. 2) may have a bearing on the possible applications of the negative n_2, and requires some further comment. The attenuation at low intensities appears to arise from cesium dimers, whose absorption band extends from the vicinity of the D lines to about 1.12 μm.[24] Using a cross section of approximately $\sigma_D \approx 4\times10^{-16}$ cm^2,[27] and concentration[28]

$$N_D = 3.54\times10^{-23} N^2 e^{5200/T(^\circ\mathrm{K})}, \tag{29}$$

we obtain the absorption coefficient $N_D\sigma_D \approx 0.017$ at $T = 460$ °C and $N = 0.32\times10^{17}$ cm^{-3}. The small signal transmission for a 100-cm path length is then approximately 18%. If N is actually smaller by a factor of about 2, as we suggested above, then the transmission would be approximately 65%. The increase in transmission with intensity up to about 3 GW/cm^2 is apparently due to either bleaching[27] or hole-burning effects in the dimers. Evidence for this is shown in Fig. 2, where one pair of points corresponds to a double pulse with a 3-nsec separation. The first pulse, whose energy density was 200 mJ/cm^2, was virtually unattenuated. It apparently bleached out the dimers, however, because the second pulse, whose density was 40 mJ/cm^2 (indicated in Fig. 2 by the cross), had significantly higher transmission than other pulses of comparable magnitude.

One is tempted to ascribe the losses at high intensities to two-photon absorption or multiphoton ionization; however, the theoretical cross sections for these processes do not support such explanations. The two-photon cross section $\sigma^{(2)}(1.064\ \mu\text{m})$, which stems primarily from the $6s$-$7s$ contribution, is approximately $3.3\times10^{-49} NI$,[23] where intensity I is measured in W/cm^2. For $N = 0.32\times10^{17}$ cm^{-3} and incident intensity $I = 3\times10^{10}$, the maximum absorption coefficient is $N\sigma^{(2)}(1.06\ \mu\text{m}) \simeq 10^{-5}$ cm^{-1}. The three-photon absorption is also negligible. One can estimate the four-photon ionization cross section from calculations carried out by Morton[29] for $\lambda = 1.0590\ \mu$m. Morton's results correspond to a cross section $\sigma^{(4)}(1.059\ \mu\text{m}) \simeq 3.7\times10^{-49} I^3$;[23] however, this number is strongly enhanced by a nearly exact resonance between 3ω and the $6f$ levels around 28 329.7 cm^{-1}. The detuning is only ≈ 1 cm^{-1}, whereas for 1.064 μm, it is 134 cm^{-1}; hence $\sigma^{(4)}(1.064\ \mu\text{m}) \simeq (1/134)^2\sigma^{(4)}(1.059\ \mu\text{m}) \simeq 2.1\times10^{-53} I^3$, giving a maximum absorption coefficient of 1.8×10^{-5} cm^{-1} for $N = 0.32\times10^{17}$ cm^{-3}. With beam spreading (and thus lowering of the intensities and cross sections), the absorption over 100 cm is negligible.

The flattening of the high-power pulses, as shown in Fig. 3(a), suggests that dimer absorption could also be responsible for the attenuation at these as well as at the lower powers. To see this, we assume for the moment that the constant-shape approximation remains valid, even when the beam spreading is large. If this were valid [and $P(t) \gg P_c$], then Eq. (27) would reduce to $a^2(t) \simeq (\lambda z/2\pi a_0)^2 P(t)/P_c$; hence the on-axis intensity $I(0) \simeq (2\pi a_0/\lambda z)^2 P_c/\pi$ would remain independent of the total power $P(t)$. However, because the flattening does occur and becomes more prominent as $P(t)$ increases, it is evident that the intensity $I(0,t)$ can actually *decrease* as $P(t)$ increases. The central portion of the beam may therefore become more susceptible to dimer absorption under these conditions.

In future papers, we will report on additional defocusing measurements using longer pulses to observe the integral terms, and on investigations of the higher-power transmission under conditions where beam flattening is negligible. We will also report on both theoretical and experimental studies of the application of cesium vapor for compensation of self-focusing and self–phase-modulation in high-power laser systems.

ACKNOWLEDGMENTS

We thank Hans Griem, John McMahon, and Raymond Elton for useful and informative discussions.

APPENDIX

To obtain the solution of Eqs. (3), we use the harmonic expansions of $\rho^{(n)}_{\alpha\beta}(t)$, as in Eq. (5); i.e.,

$$\rho^{(3)}_{\alpha\beta}(t) = \tfrac{1}{2}\sigma^{(3)}_{\alpha\beta}(\omega,t)e^{-i\omega t} + \tfrac{1}{2}\sigma^{(3)}_{\alpha\beta}(-\omega,t)e^{i\omega t} + (\text{third-harmonic terms}), \quad \text{(A1a)}$$

$$\rho^{(2)}_{\alpha\beta}(t) = \sigma^{(2)}_{\alpha\beta}(0,t) + \tfrac{1}{2}\sigma^{(2)}_{\alpha\beta}(2\omega,t)e^{-2i\omega t} + \tfrac{1}{2}\sigma^{(2)}_{\alpha\beta}(-2\omega,t)e^{2i\omega t}, \quad \text{(A1b)}$$

$$\rho^{(1)}_{\alpha\beta}(t) = \tfrac{1}{2}\sigma^{(1)}_{\alpha\beta}(\omega,t)e^{-i\omega t} + \tfrac{1}{2}\sigma^{(1)}_{\alpha\beta}(-\omega,t)e^{i\omega t}, \quad \text{(A1c)}$$

where the amplitudes $\sigma^{(n)}_{\alpha\beta}(n'\omega,t) = [\sigma^{(n)}_{\beta\alpha}(-n'\omega,t)]^*$ vary in times on the order of the pulse width t_p. Substituting Eqs. (A1) into (3) (and dropping the time label for brevity), one obtains

$$\dot\sigma^{(3)}_{\alpha\beta}(\omega) + i(\omega_{\alpha\beta} - \omega - i\Gamma_{\alpha\beta})\sigma^{(3)}_{\alpha\beta}(\omega) = i\mathcal{E}(-\omega)\hat\epsilon^*\cdot\vec S^{(2)}_{\alpha\beta}(2\omega) + 2i\mathcal{E}(\omega)\hat\epsilon\cdot\vec S^{(2)}_{\alpha\beta}(0), \quad \text{(A2a)}$$

$$\dot\sigma^{(2)}_{\alpha\beta}(2\omega) + i(\omega_{\alpha\beta} - 2\omega - i\Gamma_{\alpha\beta})\sigma^{(2)}_{\alpha\beta}(2\omega) = i\mathcal{E}(\omega)\hat\epsilon\cdot\vec S^{(1)}_{\alpha\beta}(\omega), \quad \text{(A2b)}$$

$$\dot\sigma^{(2)}_{\alpha\beta}(0) + i(\omega_{\alpha\beta} - i\Gamma_{\alpha\beta})\sigma^{(2)}_{\alpha\beta}(0) = \tfrac{1}{2}i\mathcal{E}(-\omega)\hat\epsilon^*\cdot\vec S^{(1)}_{\alpha\beta}(\omega) + \tfrac{1}{2}i\mathcal{E}(\omega)\hat\epsilon\cdot\vec S^{(1)}_{\alpha\beta}(-\omega), \quad \omega_{\alpha\beta}\neq 0, \quad \text{(A2c)}$$

$$\dot\sigma^{(2)}_{\alpha\alpha}(0) + W_\alpha\sigma^{(2)}_{\alpha\alpha}(0) - \sum_{\beta\neq\alpha} W_{\beta\alpha}\sigma^{(2)}_{\beta\beta}(0) = \mathrm{Re}[i\mathcal{E}(-\omega)\hat\epsilon^*\cdot\vec S^{(1)}_{\alpha\alpha}(\omega)], \quad \text{(A2d)}$$

$$\dot\sigma^{(1)}_{\alpha\beta}(\omega) + i(\omega_{\alpha\beta} - \omega - i\Gamma_{\alpha\beta})\sigma^{(1)}_{\alpha\beta}(\omega) = (i/\hbar)\mathcal{E}(\omega)\hat\epsilon\cdot\vec\mu_{\alpha\beta}(\delta_{\beta 0} - \delta_{\alpha 0}), \quad \text{(A2e)}$$

where

$$\vec S^{(n)}_{\alpha\beta}(n'\omega) \equiv \frac{1}{2\hbar}\sum_\gamma [\vec\mu_{\alpha\gamma}\sigma^{(n)}_{\gamma\beta}(n'\omega) - \sigma^{(n)}_{\alpha\gamma}(n'\omega)\vec\mu_{\gamma\beta}], \quad \text{(A3)}$$

and $\Gamma_{\alpha\beta}$, W_α, and $W_{\beta\alpha}$ are the phase relaxation and collisional mixing rates described in the text.

With the exception of (A2d), all of the equations (A2) have the general form

$$\dot\sigma(t) + (i\Omega + \Gamma)\sigma(t) = R(t), \quad |\Omega| \gg \Gamma, \quad \text{(A4)}$$

with the formal solution for $\sigma(-\infty) = R(-\infty) = 0$,[30]

$$\sigma(t) = \int_{-\infty}^{t} dt'\, e^{-(i\Omega+\Gamma)(t-t')}R(t') = -\sum_{m=0}^{\infty}\left(\frac{-1}{i\Omega+\Gamma}\right)^{m+1}\frac{d^mR(t)}{dt^m}. \quad \text{(A5)}$$

For example, (A2e) yields the result

$$\sigma^{(1)}_{\alpha\beta}(\omega,t) = -\frac{i}{\hbar}(\delta_{\beta 0} - \delta_{\alpha 0})\hat\epsilon\cdot\vec\mu_{\alpha\beta} \times \sum_{m=0}^{\infty}\left(\frac{-1}{i(\omega_{\alpha\beta}-\omega)+\Gamma_{\alpha\beta}}\right)^{m+1}\frac{\partial^m\mathcal{E}(\omega,t)}{\partial t^m}. \quad \text{(A6)}$$

Since Ω represents quantities such as $\omega_{\alpha\beta}$, 2ω, $\omega_{\alpha\beta}\pm\omega$, or $\omega_{\alpha\beta}\pm 2\omega$, but $|(1/R)\,dR/dt|$ is on the order of the laser linewidth, postulate (ii) leads to the condition $|(1/R)(dR/dt| \ll \Omega$; hence it is necessary to retain only the lowest-order terms of (A5) and (A6).

Equation (A2d) may be rewritten by substituting (A3) and expansion (A6). Retaining only the zero- and first-derivative terms of (A6), and noting that $\Gamma_{\beta\alpha} = \Gamma_{\alpha\beta}$, one obtains

$$\dot\sigma^{(2)}_{\alpha\alpha}(0,t) + W_\alpha\sigma^{(2)}_{\alpha\alpha}(0,t) - \sum_{\beta\neq\alpha} W_{\beta\alpha}\sigma^{(2)}_{\beta\beta}(0,t) \simeq \frac{1}{4\hbar^2}\sum_\beta(\delta_{\beta 0} - \delta_{\alpha 0})\left[\left(\frac{|\hat\epsilon\cdot\vec\mu_{\beta\alpha}|^2}{i(\omega_{\beta\alpha}-\omega-i\Gamma_{\beta\alpha})} + \frac{|\hat\epsilon\cdot\vec\mu_{\alpha\beta}|^2}{i(\omega_{\alpha\beta}-\omega-i\Gamma_{\beta\alpha})}\right)\mathcal{E}(-\omega,t)\mathcal{E}(\omega,t) + \left(\frac{|\hat\epsilon\cdot\vec\mu_{\beta\alpha}|^2}{(\omega_{\beta\alpha}-\omega-i\Gamma_{\beta\alpha})^2} + \frac{|\hat\epsilon\cdot\vec\mu_{\alpha\beta}|^2}{(\omega_{\alpha\beta}-\omega-i\Gamma_{\beta\alpha})^2}\right)\mathcal{E}(-\omega,t)\frac{\partial\mathcal{E}(\omega,t)}{\partial t}\right] + \text{c.c.} \quad \text{(A7a)}$$

$$\simeq \sum_\beta(\delta_{\beta\alpha} - \delta_{\alpha 0})R_\beta\left(\Gamma_{\beta 0}\langle E^2(t)\rangle + \frac{\frac{1}{2}\,d\langle E^2(t)\rangle}{dt}\right), \quad \text{(A7b)}$$

where $\langle E^2(t)\rangle = \frac{1}{2}|\mathcal{E}(\omega,t)|^2$, R_β is defined by Eq. (9c), and postulate (ii) has been used to justify the neglect of $\Gamma_{\beta 0}$ in the denominator of R_β. Although the zero-derivative term is the largest contribution to (A6), it is evident that the corresponding term $\Gamma_{\beta 0}\langle E^2(t)\rangle$ in (A7b) may be comparable to or less than the first-derivative contribution $\frac{1}{2}\, d\langle E^2(t)\rangle/dt$. This results from the fact that the largest portions of the zero-derivative terms in (A7a) cancel when they combine with their complex conjugates. If we define the variable $q_\alpha(t)$ by the relation

$$\sigma^{(2)}_{\alpha\alpha}(0,t) = \frac{1}{2}\sum_\beta (\delta_{\beta\alpha} - \delta_{\alpha 0}) R_\beta \langle E^2(t)\rangle + q_\alpha(t)\,, \tag{A8}$$

then Eq. (A7b) leads immediately to Eqs. (11) and (12).

The near cancellation of the zero-derivative terms occurs only in the evaluation of Eq. (A2d). In the solution of Eqs. (A2a)–(A2c) and (A2e), one can therefore use postulate (ii) to omit all but the zeroth term of (A5), and to ignore all $\Gamma_{\alpha\beta}$ factors. The resulting solutions

$$\sigma^{(3)}_{\alpha\beta}(\omega,t) \simeq \frac{\mathcal{E}(-\omega,t)\hat{\epsilon}^*\cdot\vec{s}^{(2)}_{\alpha\beta}(2\omega,t) + 2\mathcal{E}(\omega,t)\hat{\epsilon}\cdot\vec{s}^{(2)}_{\alpha\beta}(0,t)}{\omega_{\alpha\beta}-\omega}\,, \tag{A9a}$$

$$\sigma^{(2)}_{\alpha\beta}(2\omega,t) \simeq \frac{\mathcal{E}(\omega,t)\hat{\epsilon}\cdot\vec{s}^{(1)}_{\alpha\beta}(\omega,t)}{\omega_{\alpha\beta}-2\omega}\,, \tag{A9b}$$

$$\sigma^{(2)}_{\alpha\beta}(0,t) \simeq \frac{\mathcal{E}(-\omega,t)\hat{\epsilon}^*\cdot\vec{s}^{(1)}_{\alpha\beta}(\omega,t) + \mathcal{E}(\omega,t)\hat{\epsilon}\cdot\vec{s}^{(1)}_{\alpha\beta}(-\omega,t)}{2\omega_{\alpha\beta}}\,, \tag{A9c}$$

$$\omega_{\alpha\beta}\neq 0\,,$$

$$\sigma^{(1)}_{\alpha\beta}(\omega,t) \simeq \frac{\mathcal{E}(\omega,t)\hat{\epsilon}\cdot\vec{\mu}_{\alpha\beta}(\delta_{\beta 0}-\delta_{\alpha 0})}{\hbar(\omega_{\alpha\beta}-\omega)}\,, \tag{A9d}$$

along with the instantaneous portion of (A8), are equivalent to those obtained from ordinary perturbation theory.[13–15] Combining these results with expression (6), one obtains Eqs. (7)–(10) after some tedious but straightforward algebra.

*Work supported jointly by the Defense Advanced Research Projects Agency, ARPA Order No. 2694, and the U.S. Energy Research and Development Administration.

[1]D. Grischkowsky, Phys. Rev. Lett. 24, 866 (1970).
[2]S. A. Akhmanov, A. I. Kovrigin, S. A. Maksimov, and V. E. Ogluzdin, Zh. Eksp. Teor. Fiz. Pis'ma Red. 15, 186 (1972) [JETP Lett. 15, 129 (1972)].
[3]J. E. Bjorkholm and A. Ashkin, Phys. Rev. Lett. 32, 129 (1974).
[4]S. A. Bakhramov, U. G. Gulyamov, K. N. Drabovich, and Ya. Z. Faizullaev, Zh. Eksp. Teor. Fiz. Pis'ma Red. 21, 229 (1975) [JETP Lett. 21, 102 (1975)].
[5]D. Grischkowsky and J. A. Armstrong, Phys. Rev. A 6, 1566 (1972).
[6]V. M. Artyunyan, N. N. Badalyn, V. A. Iradyan, and M. E. Movsesyan, Zh. Eksp. Teor. Fiz. 58, 37 (1970) [Sov. Phys.-JETP 31, 22 (1970)].
[7]D. Grischkowsky, E. Courtens, and J. A. Armstrong, Phys. Rev. Lett. 31, 422 (1973).
[8]R. H. Lehmberg, J. Reintjes, and R. C. Eckhardt, Appl. Phys. Lett. 25, 374 (1974).
[9]P. D. Maker and R. W. Terhune, Phys. Rev. 137, A801 (1965).
[10](a) R. Speck and E. Bliss, Lawrence Livermore Laboratory Semiannual Report, Jan.–June 1973 (unpublished); (b) A. Owyoung, *Symposium on Laser Induced Damage in Optical Materials*, Nat. Bur. Stand. Special Publication 387 (U.S. GPO, Washington, D.C., 1973); (c) M. J. Moran, C. Y. She, and R. L. Carman, IEEE J. Quantum Electron. QE-11, 259 (1975).
[11]V. S. Butylkin, A. E. Kaplan, and Yu. G. Khronopulo, Zh. Eksp. Teor. Fiz. 59, 921 (1970) [Sov. Phys.-JETP 32, 501 (1971)].
[12]S. A. Akhmanov, R. V. Khokhlov, and A. P. Sukhorukov, in *Laser Handbook*, edited by F. T. Arecchi and E. O. Schulz-Dubois (North-Holland, Amsterdam, 1972), Vol. 2.
[13]J. A. Armstrong, N. Bloembergen, J. Ducuing, and P. S. Pershan, Phys. Rev. 127, 1918 (1962).
[14]B. J. Orr and J. F. Ward, Mol. Phys. 20, 513 (1971).
[15]P. W. Langhoff, S. T. Epstein, and M. Karplus, Rev. Mod. Phys. 44, 602 (1972).
[16]R. Bernheim, *Optical Pumping, An Introduction* (Benjamin, New York, 1965).
[17]P. R. Berman and W. E. Lamb, Jr., Phys. Rev. 187, 221 (1969); C. G. Carrington, D. N. Stacey, and J. Cooper, J. Phys. B 6, 417 (1973).
[18]C. E. Moore, *Atomic Energy Levels*, Nat. Bur. Stand. (U.S. GPO, Washington, D.C., 1958), Vol. III.
[19]J. T. Fournier and E. Snitzer, IEEE J. Quantum Electron. QE-10, 473 (1974).
[20]R. H. Lehmberg and J. Reintjes, Bull. Am. Phys. Soc. 20, 635 (1975); Phys. Rev. A 12, 2574 (1975).
[21]P. P. Bey and H. Rabin, Phys. Rev. 162, 794 (1967).
[22]O. S. Heavens, J. Opt. Soc. Am. 51, 1058 (1961). This particular set of matrix elements was chosen because the corresponding oscillator strengths come closer to satisfying the Thomas-Kuhn sum rule than those tabulated elsewhere. For example, the total $6s$–$6p$ oscillator strength is $f(6s,6p)=1.05$, whereas the value given in the tables of Ref. 23 is 1.13.
[23]R. B. Miles and S. E. Harris, IEEE J. Quantum Electron. QE-9, 470 (1973).
[24]D. S. Bayley, E. C. Eberlin, and J. H. Simpson, J. Chem. Phys. 49, 2863 (1968).
[25]This was obtained by taking the weighted average of the $6p\,^2P_{1/2}$ and $6p\,^2P_{3/2}$ linewidths measured by C. L. Chen and A. V. Phelps, Phys. Rev. 173, 62 (1968).
[26]*Handbook of Tables for Applied Engineering Science*, edited by R. E. Bolz and G. L. Tuve (Chemical Rubber, Cleveland, 1970).
[27]P. P. Sorokin and J. R. Lankard, IEEE J. Quantum Electron. QE-8, 813 (1972).
[28]M. Lapp and L. P. Harris, J. Quant. Spectrosc. Radiat. Transfer 6, 169 (1966).
[29]V. M. Morton, Proc. Phys. Soc. Lond. 92, 301 (1967).
[30]M. D. Crisp, Phys. Rev. A 8, 2128 (1973).

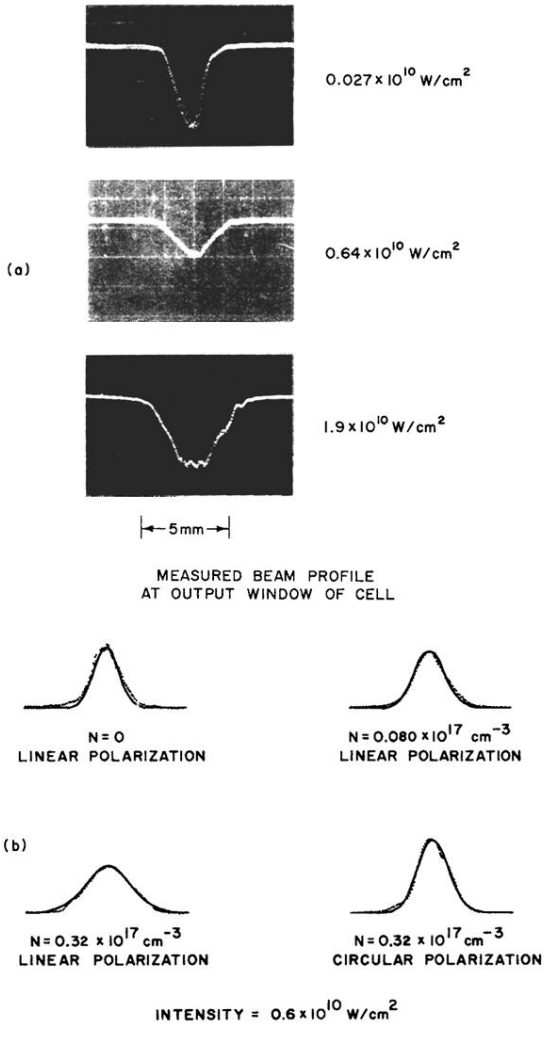

FIG. 3. Spatial profiles of the pulse at the exit window of the Cs cell. (a) Oscilloscope traces of photodiode array measurement at low, intermediate, and high intensity. (b) Comparison between theoretical profiles (solid lines) and typical measured profiles (dotted lines) at intermediate pulse energies.